Theoretical investigation of the increase in the Rosseland mean opacity for hot dense mixtures

Jun Yan and Ze-Qing Wu
Institute of Applied Physics and Computational Mathematics, Beijing 100088, China
(Received 11 January 2002; published 10 June 2002)

Based on a detailed configuration accounting model with the term structures treated by the unresolved transition array model, a large scale calculation has been performed for the opacities of medium- and high-*Z* materials and mixtures. Agreement between our calculated results and previous theoretical simulations is obtained. By filling in the low-opacity regions of one material with the high-opacity regions of other materials, the Rosseland mean opacity of their combination will be increased. This should be of great interest to hohlraum design in indirect-drive inertial confinement fusion. Based on our studies, many mixtures, such as Au+Nd, or Ho+Sn, can result in a similar (or higher) increase in the Rosseland mean as the previously proposed Au +Gd mixture.

DOI: 10.1103/PhysRevE.65.066401 PACS number(s): 52.25.Os, 52.25.Vy

I. INTRODUCTION

In the indirect approach to inertial confinement fusion (ICF) [1,2], materials with high Rosseland mean opacity are of great interest to the hohlraum design because of their high reemission and x-ray conversion efficiency [3]. Usually, a single high-*Z* material, such as gold, is used to construct the hohlraum walls because it has a high opacity over a broad range of the x-ray spectrum. However, the absorption spectrum of gold at the hohlraum temperature, like that of any other element, is not constant. It has peaks and valleys. These valleys dominate and reduce the Rosseland mean opacity. If the valleys can be filled up by peaks of other material(s), the Rosseland mean will increase. Therefore, people try to use hohlraums of mixed materials. In the early 1990s, Nishimura *et al.* studied the increase in the Rosseland mean opacity of mixtures [4]. They attempted to quantify the effect by measure the efficiency of various mixtures of materials in converting laser light to x rays and inferring, from these data, the change in opacity. Recently, the Rosseland mean opacity of a mixture of Au and Gd at high temperatures was directly measured by Orzechowski and co-workers [5]. An increase of more than 40% in the Rosseland mean opacity over that of pure gold was observed. A theoretical simulation was also carried out using the opacity code XSN [6] in their work [5].

The Rosseland mean opacity calculation is controlled by the details of the frequency-dependent opacity. To obtain accurate results, the key point is to calculate a frequency-dependent opacity which displays the saw tooth features as accurately as possible. The theoretical calculation of accurate frequency-dependent opacity is a challenging task for high-*Z* plasmas at high temperature and density. It requires a huge amount of atomic data. Usually, the average atom (AA) model is used to calculated the opacity of medium- and high-*Z* mixtures as in Refs. [5,7]. Only a few works have been carried out based on methods beyond the level of the AA model. Using the supertransition array (STA) method, Colombant and co-workers have performed an extensive calculation of opacities for mixtures of Au and other elements [8]. Further theoretical work on the opacity of the mixtures Au +Gd and Au+Sm, using an unresolved transition array (UTA) model [9,10], has also been presented [11]. In a previous paper [12], we presented the calculated opacity for a mixture of gold and gadolinium at the temperature 250 eV and three densities 0.1, 1.0, and 10.0 g/cm^3. Agreement between our theoretical results and the experimental measurements as well as the theoretical simulations of the STA method was obtained. The present work can be regarded as a sequel to our previous paper [12], and we will report a more extensive investigation for the opacities of mixed materials.

II. THEORETICAL CALCULATIONS

The present calculations are based on the detailed configuration accounting (DCA) model, in which the term structures are treated by the UTA model [9,10]. Since detailed descriptions of our DCA/UTA method have been given elsewhere [12–15], here we only emphasize the following three points. (i) In order to include as many important configurations as possible in the opacity calculation, we use the self-consistent-field (SCF) energy levels database to investigate and produce important configurations. The database is constructed from the energy level and quantum defects of some bound orbitals and continuum orbitals, which have already been calculated before from the self-consistent-field method and are arranged within different channels for all ionic stages of an element. Then we construct a huge amount of configurations (up to eight electrons excited from all shells). The database is used to calculate the average energy of the configuration approximately. By comparing their Boltzmann factors, we choose the most important configurations to be included in solving the Boltzmann-Saha equations and the calculations of properties for photoexcitation and photoionization processes. This can ensure the convergence of the calculation results, i.e., both the average charge and the opacity spectrum, for most cases, within 1%. (ii) We use a DCA model, but with term splitting effects included using an UTA model [9,10] assuming *j-j* coupling. The UTA model treats the superposition of many overlapping, intrinsically broadened bound-bound transitions resulting from two electronic configurations as a single spectral feature. Each configuration-configuration transition array is then characterized by average quantities such as total intensity, average

transition energy, and variance. In our calculation, the transition energies, oscillator strength, and variance are evaluated using the relativistic wave functions obtained based on the Dirac-Slater SCF potential. Atomic configuration populations are calculated assuming local thermodynamic equilibrium (LTE) by solving the well-known Boltzmann-Saha equations. (iii) Atomic data are calculated within the framework of quantum defect theory (QDT) [16–20]. In hot dense LTE plasmas, there exist a huge number of configurations with high principal quantum numbers. QDT is a powerful method to treat these configurations. In this method, the physical quantities show smooth properties and can be treated in a unified manner within channels [21,22]. Therefore, we can perform interpolations (rather than extrapolations) to reduce the computational effort.

Including these features described above, we have developed a computer code to provide opacity data. The validity of our DCA/UTA method has been proved. For both the spectral-resolved opacities [13–15] and the Rosseland mean [12], good agreement is obtained between our calculated results and the experimental measurements as well as other theoretical simulations. In the present work, we have calculated the opacities of the following medium- and high-Z elements and their mixtures: Co, Ni, Cu, Ag, Sn, Cs, Nd, Sm, Gd, Ho, W, and Au. In practical calculation, Cs is replaced by its iodide (CsI) because cesium is liquid at room temperature and CsI has almost the same spectrum as Cs. When producing configurations, we cut off those configurations with high principal quantum number n greater than 10. For each ionic stage of an element, we choose about 10 000 most important configurations from a huge number of configurations, and, for an element, 200 000 or more configurations are included. For each configuration, all possible bound-bound transitions from $1s,2s,2p_-,2p_+,\ldots,5f_-,5f_+$ initial orbitals to ''all'' final orbitals ($n \leqslant 10$) are taken into account. The calculated results will be given in the following sections.

III. RESULTS AND DISCUSSION

As mentioned in the Introduction, pure gold is typically used to construct the hohlraum walls in indirectly driven ICF. In order to improve the Rosseland mean opacity, Orzechowski *et al.* proposed mixing gadolinium with gold [5]. In fact, many medium- and high-Z materials would be good choices because their absorption peaks can overlap the windows in the Au spectrum as well as or better than Gd. Figure 1 displays the frequency-dependent opacities of three typical medium- and high-Z elements: Ni, Sn, and Nd at the typical hohlraum temperature of 250 eV and density of 1 g/cm^3. The spectrum of Au is also plotted in Fig. 1 for reference. In the spectrum of gold, the absorption peaks in the photon energy range about 500–1000 eV are helpful for the Rosseland mean at the temperature 250 eV, while the windows at about 160 eV, 400 eV, and 1000–2200 eV, especially the windows above 1000 eV, play important roles which dominate and reduce the Rosseland mean. These windows can be filled up by the absorption peaks of other elements as shown in Fig. 1. The overlap between the spectra of the high-Z elements Au and Nd seems to be the best, not only above 1000 eV, but also at photon energies about 160 eV and 400 eV. The overlap between the spectra of Au and medium-Z elements, such as Ni, seems not so good, but at photon energies around and above 1000 eV, which is most important for the Rosseland mean because it is around the maximum of the weight function at the plasma temperature 250 eV, there are big absorption peaks in the spectra of Ni and Sn. This can also result in an enhancement of the Rosseland mean opacity. Table I gives the calculated Rosseland mean opacity at the temperature 250 eV and the density 1 g/cm^3. The theoretical results of the STA method [8] are also listed in Table I for comparison.

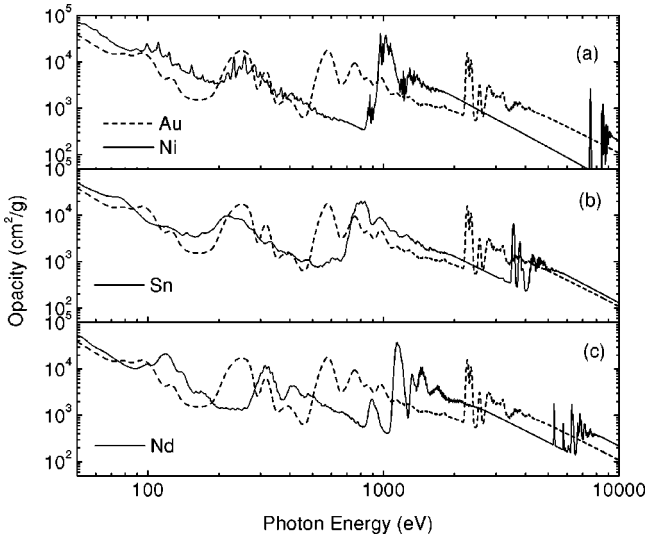

FIG. 1. Frequency-dependent opacity of Ni, Sn, Nd, and Au at a temperature of 250 eV and density of 1 g/cm^3.

The Rosseland mean opacity we calculated for pure gold at the temperature 250 eV and the density 1 g/cm^3 is slightly larger than the value from the STA method and that

TABLE I. Rosseland mean opacity κ_R(cm^2/g) for various elements and their mixtures with gold at a temperature of 250 eV and density 1 g/cm^3.

Element	κ_R of pure element		Maximum κ_R when mixed with Au		% of Au
	Present results	Results of STA [8]	Present results	Results of STA [8]	Present
Co	1224	1140	2223	2169	20
Ni	1198	1118	2340	2291	20
Cu	1035	952	2283	2263	30
Ag	1756	1844	1990	2036	20
Sn	1916	1997	2218	2280	20
CsI	2008	2056	2548	2566	20
Nd	1402	1509	2439	2475	40
Sm	1352		2286		50
Gd	1345	1377	2196	2162	60
Ho	1387		2057		70

in Ref. [5]. Our result is 1729 cm^2/g. The STA value was 1620 cm^2/g [8]. In Ref. [5], the value of 1500 cm^2/g was obtained with the XSN model, and 823 cm^2/g with another average atom model. In Table I, our calculated Rosseland mean opacities, both for the pure elements and the mixtures, are slightly larger or smaller than the corresponding results of the STA method. Note that in the STA method, the frequency-dependent opacities of each element are calculated with the same temperature and the effective densities via the same chemical potentials, and then the Rosseland mean of the mixtures is calculated with the postprocessed program MIX [8]. In the present work, however, we solve the Saha equations by including the configurations of all species, which ensures that the same electron density can be achieved for each species. Then we calculate the spectrum of the frequency-dependent opacity for the mixture, based on which the Rosseland mean can be obtained. There are two points that can affect the present calculation of the Rosseland mean. (1) The configuration interaction (CI) effects. As pointed out in Ref. [23], the CI between relativistic jj configurations pertaining to the same general (nonrelativistic) configuration can lead to noticeable changes in the opacity, especially in the detailed spectra where $\Delta n=0$, and sometimes $\Delta n=1$, and for electrons of outer shells. In the present calculation, the CI effects have not been included, but we think that the CI effects may not lead to large changes in the Rosseland mean, because in the photon energy region near the maximum of the weighted function, most transitions are to high n or from inner shells. Of course, further study is still needed to elucidate the CI effects on the Rosseland mean of high-Z mixtures. (2) The pressure ionization. At high densities, the high principal quantum number (n) orbitals are unbound. Usually, people use the ion-sphere or the Debye model to estimate n_{max}, and all configurations with high principal quantum number $n<n_{max}$ should be included in the calculation of the opacity. But considering that the number of configurations is too large, and it is difficult to calculate the wave functions for the initial configurations with high principal quantum number, we here cut off the configurations of $n>10$. (Here 10 is lower than the n_{max} that we estimated using the Debye model.) For the final configurations, we also cut off at $n>10$ although we can calculate the transitions within the framework of QDT. This should have a small effect on the calculated results of opacity, and also deserves further studies. The above mentioned two points and other different treatments may result in the discrepancies between our results and those of the STA model. However, the agreements are satisfactory. In Table I, we also give the optimum fraction of Au corresponding with the maximum Rosseland mean of the mixture in the last column. Here it should be pointed out that a slightly higher value of the Rosseland mean opacity than the corresponding maximum κ_R in Table I may be achieved by adjusting the fraction of species within $\pm 9\%$, because only mixtures with fractions of $n\times 10\%$ ($n=1,2,\ldots,9$) are considered in the present calculation. Note that in Table I the pure elements have a wide range of opacity values, and, for their mixtures, a general increase in the Rosseland mean over either of the constituents is obtained. Many elements, except Ag and Ho, have a larger value when mixed with Au than that of Au+Gd. The increases in Rosseland mean of Au+Ag and Au+Ho are not high, mainly because at photon energies around and above 1000 eV the overlap is not very good; for Ag, the absorption peaks in the spectrum are a little lower and for Ho a little higher than 1000 eV.

TABLE II. Rosseland mean opacity κ_R (cm^2/g) for various elements and mixtures. κ_R^s denotes the Rosseland mean opacity of the pure element, while κ_R^m denotes the maximum Rosseland mean obtained when mixed with Au.

Element	κ_R^s	κ_R^m	% of Au	κ_R^s	κ_R^m	% of Au
			$T_e=250$ eV			
	Density 0.1 g/cm^3			Density 10 g/cm^3		
Co	353	1102	30	2406	2987	20
Ni	368	1194	20	2479	3065	20
Cu	332	1231	30	2300	2958	20
Ag	877	1089	30	2641	2791	20
Sn	1020	1283	20	2793	3024	20
CsI	868	1420	30	3131	3405	20
Nd	763	1628	40	2483	3069	40
Sm	642	1536	50	2382	2938	50
Gd	594	1390	60	2281	2850	50
Ho	628	1264	60	2277	2750	60
Au	968			2365		
			Density 1 g/cm^3			
	$T_e=200$ eV			$T_e=300$ eV		
Co	1507	3040	20	907	1515	20
Ni	1486	3067	30	952	1664	20
Cu	1332	2920	40	860	1696	20
Ag	2909	3123	10	1155	1363	20
Sn	2689	3217	20	1244	1525	20
CsI	2553	3495	30	1465	1828	20
Nd	1813	3104	60	1259	2012	40
Sm	1826	3029	60	1151	1927	40
Gd	1845	2926	60	1073	1786	50
Ho	1953	2898	70	1055	1612	60
Au	2456			1231		

In reality, the hohlraum samples a range of densities and temperatures. The most accurate way to determine the opacity of the composite should be to simulate the experiment with rad-hydro code such LASNEX [5,11] or LARED [24]. In the present work, we carried out the simulation with our LTE DCA/UTA code by calculating the opacity at several temperatures and densities: at the temperature of 250 eV and two densities of 0.1 g/cm^3 and 10 g/cm^3, and at the two temperatures of 200 eV and 300 eV and the density of 1 g/cm^3. The calculated results are listed in Table II. At low temperature and/or high density, the Rosseland means of many mixtures are higher than those of Au+Gd, which happened at the temperature of 250 eV and the density of 1 g/cm^3. This is not the case at high temperature and/or low density. However, the Rosseland mean opacities of Au+Nd mixtures are always higher than those of Au+Gd mixtures. This suggests that the Au+Nd mixture is a better choice than the Au+Gd mixture suggested in Ref. [5].

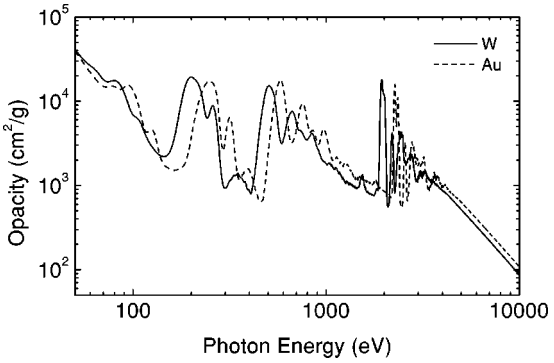

FIG. 2. Frequency-dependent opacity of W and Au at a temperature of 250 eV and density of 1 g/cm^3.

In addition to the above results, we have performed a more extensive investigation for the opacities of other mixtures. First, we mixed tungsten with the above ten medium- and high-Z elements. We chose tungsten because, like Au, it also has a high opacity over a broad range of the x-ray spectrum, since tungsten is close to and only a little lower than gold in the periodic table of elements. Figure 2 displays the frequency-dependent opacities of tungsten and gold at the temperature 250 eV and the density of 1 g/cm^3. The absorption peaks from the O-, N-, and M-shell electrons of tungsten are in lower-photon-energy regions than those of gold, which may result in a higher Rosseland mean opacity than Au at lower hohlraum temperatures, for example, around or lower than 150 eV. The opacity of materials at lower temperatures than 200 eV will not be reported in the present paper. Here we mainly focus our interest on the hohlraum temperature range around 250 eV. In Table III, we give the calculated Rosseland mean opacities for various mixtures with tungsten. At the density of 1 g/cm^3 and three temperatures of 200, 250, and 300 eV, the Rosseland mean opacities of pure tungsten are 2288, 1562, and 1121 cm^2/g, respectively, which are all smaller than the corresponding values for Au. For some mixtures, such as Ag+W, Sn+W, and CsI+W, the Rosseland means are always larger than the corresponding values of mixtures with Au. This may be because for these cases, the absorption peaks of Ag, Sn, and CsI around

TABLE III. The maximum Rosseland mean opacity κ_R^m (cm^2/g) for various mixtures with W.

Element	κ_R^m	% of W	κ_R^m	% of Wu	κ_R^m	% of W
	$T_e=200$ eV		$T_e=250$ eV		$T_e=300$ eV	
Co	3064	30	2290	20	1566	20
Ni	2993	30	2333	20	1692	20
Cu	2789	40	2198	30	1660	30
Ag	3256	20	2098	20	1441	20
Sn	3400	20	2351	20	1610	30
CsI	3567	30	2645	30	1907	30
Nd	2860	60	2278	50	1895	40
Sm	2728	60	2100	60	1761	50
Gd	2652	70	1930	60	1593	60
Ho	2527	70	1759	70	1337	60

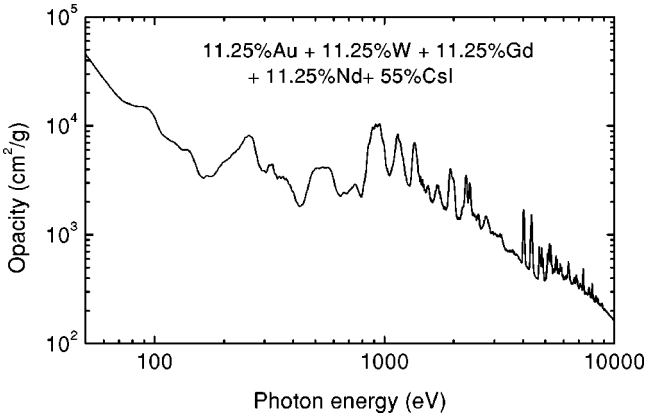

FIG. 3. Frequency-dependent opacity of the 11.25%Au +11.25%W+11.25%Gd+11.25%Nd+55.0%CsI mixture at a temperature of 250 eV and density of 1 g/cm^3. Note that a large absorption ''peak'' is formed around 1 keV.

1 keV play the dominant role, and the overlap between their spectra and the spectrum of W (whose absorption peaks are in a lower photon energy region than those of Au), can form a bigger absorption ''peak'' around 1 keV.

In order to find an empirical upper bound to the Rosseland mean, we calculated the opacity for mixtures of multielements. In Ref. [8], the best results at the temperature of 250 eV and the density of 1 g/cm^3 are 2715 cm^2/g for a mixture of three elements 24%Au+20%Gd+56%CsI, and 2844 cm^2/g for a mixture of four elements 15%Au +25%Gd+35%CsI+25%Ag. Our calculated result, for the first case, is slightly larger than the value of the STA method, 2792 cm^2/g. But for the second case, we find that by adding Ag only a very small increase, to the value of 2808 cm^2/g, is obtained. In fact, for the mixture of three elements, by slightly adjusting the fraction of elements to 22.5%Au +22.5%Gd+55%CsI, a value of the Rosseland mean of 2804 cm^2/g can also be achieved. In Fig. 2, the absorption peaks and valleys of Au and W overlap each other in the photon energy range from 500 to 1000 eV, especially around 585 and 660 eV. This stimulates us to use Au+W instead of pure Au. A relatively larger increase, 2902 cm^2/g, is obtained for the mixture of 11.25%Au+11.25%W +22.5%Gd+55.0%CsI. Similarly, we use Gd+Nd instead of pure Gd, and a slight increase 2944 cm^2/g is obtained for the mixture of 11.25%Au+11.25%W+11.25%Gd +11.25%Nd+55.0%CsI. Figure 3 displays the frequency-dependent opacity of the above mixture. Note that around 1 keV a global absorption ''peak'' is formed. To improve upon this mixture, other elements whose absorption peaks can fill in the gaps in Fig. 3 may be added, and a slight enhancement may be achieved.

Although the above well chosen multielement mixture allows us to obtain an upper bound in opacity, it will probably not be feasible for a variety of reasons. Let us return to a mixture of two elements, which may be more feasible. In our calculation, we find that the spectra of some elements other than Au and W can also overlap each other as well as or better than the above mentioned two-element mixtures. Figure 4 displays the frequency-dependent opacities of Ho, Sn,

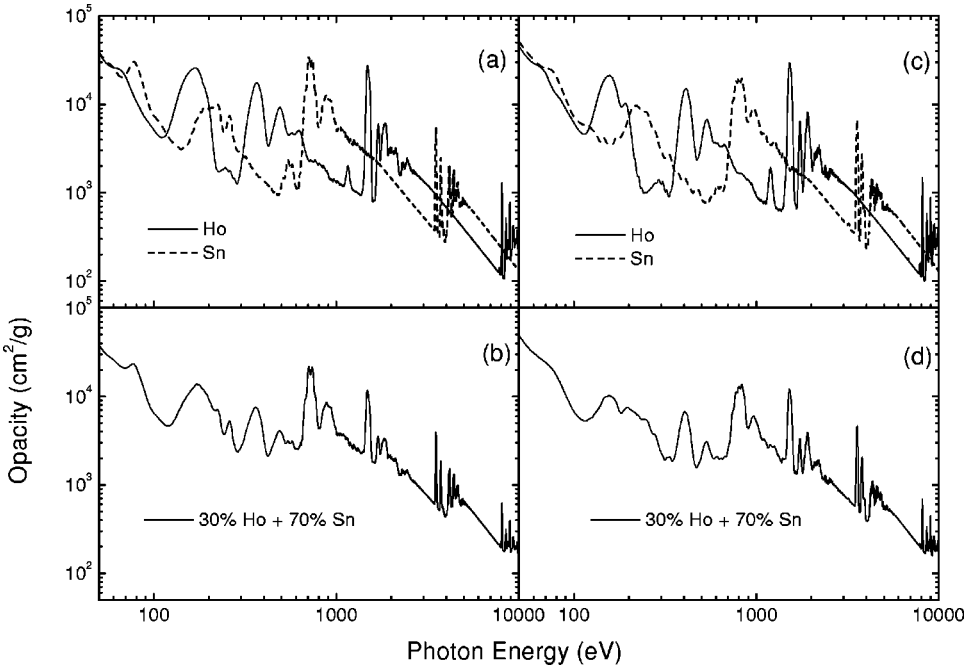

FIG. 4. Frequency-dependent opacity of Sn, Ho, and Ho+Sn mixture.

and their mixture at the density of 1 g/cm^3 and the temperatures of 200 and 250 eV. It can be seen that the overlap between the peaks and valleys in the spectra of Ho and Sn is very good in an extensive photon energy range like that of Au+Nd in Fig. 1(c). Therefore, large values of the Rosseland mean are obtain for their mixtures: 3514 cm^2/g at 200 eV (70%Sn+30%Ho), 2497 cm^2/g at 250 eV (70%Sn +30%Ho), and 1793 cm^2/g at 300 eV (60%Sn+40%Ho). These values are larger than most of the corresponding values in Tables I–III, which suggests that the mixture of Ho +Sn is also a good candidate for constructing the hohlraum wall.

Finally, we conclude as follows. Based on the DCA/UTA method, we have carried out an extensive calculation of the opacity for many materials and mixtures. The increase in Rosseland mean opacity was investigated. Based on our studies, many mixtures can result in a similar or higher increase in the Rosseland mean than Au+Gd. The Au+Nd and Ho+Sn mixtures are especially suggested for constructing hohlraum walls because of their high Rosseland mean. An upper bound for the Rosseland mean, the value 2944 cm^2/g for a multielement mixture, compared to the value of 1729 cm^2/g of pure gold at 250 eV and 1 g/cm^2, was also provided.

ACKNOWLEDGMENTS

We thank Professor Jia-Ming Li and Dr. Jia-Min Yang for helpful discussions. This work is supported by the National Science Foundation of China under Grant Nos. 10174009 and 10074062, the National High-Tech ICF Committee of China, and the Science and Technology Funds of CAEP under Grant No. 20010218.

[1] J.D. Lindl, R.L. McCrory, and E.M. Campbell, Phys. Today **45** (9), 32 (1992).
[2] J.H. Nuckolls, L. Wood, A. Thiessen, and G.B. Zimmerman, Nature (London) **239**, 129 (1972).
[3] M.D. Rosen, Phys. Plasmas **3**, 1803 (1996).
[4] H. Nishimura, T. Endo, H. Shigara, Y. Kato, and S. Nakai, Bull. Am. Phys. Soc. **37**, 1383 (1992); Appl. Phys. Lett. **62**, 1344 (1993).
[5] T.J. Orzechowski, M.D. Rosen, H.N. Kornblum, J.L. Porter, L.J. Suter, A.R. Thiessen, and R.J. Wallace, Phys. Rev. Lett. **77**, 3545 (1996).
[6] W.A. Lokke and W.H. Grasberger, Lawrence Livermore National Laboratory Report No. UCRL-52276 1977 (unpublished).
[7] N.K. Gupta and B.K. Godwal, Laser Part. Beams **19**, 1 (2001).
[8] D. Colombant, M. Klapisch, and A. Bar-Shalom, Phys. Rev. E **57**, 3411 (1998).
[9] C. Bauche-Arnoult, J. Bauche, and M. Klapisch, Phys. Rev. A **20**, 2424 (1979); **25**, 2641 (1982); **30**, 3026 (1984); **31**, 2248 (1985).
[10] A. Bar-Shalom, J. Oreg, W.H. Goldstein, D. Shvarts, and A. Zigler, Phys. Rev. A **40**, 3183 (1989); Phys. Rev. E **51**, 4882 (1995).
[11] P. Wang, J.J. MacFarlane, and T.J. Orzechowski, Rev. Sci. Instrum. **68**, 1107 (1997).
[12] Jun Yan and Yu-Bo Qiu, Phys. Rev. E **64**, 056401 (2001).
[13] Jun Yan, Yi-Zhi Qu, and Jia-Ming Li, High Power Laser Part. Beams (China) **11**, 65 (1999).
[14] Jun Yan and Jia-Ming Li, Chin. Phys. Lett. **17**, 194 (2000).
[15] Jia-Ming Li, Jun Yan, and Yong-Lun Peng, Radiat. Phys.

Chem. **59**, 181 (2000).
[16] M.J. Seaton, Proc. Phys. Soc. London **88**, 801 (1966); Rep. Prog. Phys. **46**, 167 (1983).
[17] U. Fano, Phys. Rev. A **2**, 353 (1970); J. Opt. Soc. Am. **65**, 979 (1975).
[18] C.M. Lee (Jia-Ming Li), Phys. Rev. A **10**, 584 (1974); Acta Phys. Sin. **29**, 419 (1980).
[19] C. Greene, U. Fano, and G. Strinati, Phys. Rev. A **19**, 1485 (1979).
[20] Jun Yan, Yi-Zhi Qu, Lan Voky, and Jia-Ming Li, Phys. Rev. A **57**, 997 (1998).
[21] Jian-Guo Wang, Yi-Zhi Qu, and Jia-Ming Li, Phys. Rev. A **52**, 4274 (1995).
[22] Jian-Guo Wang, Xiao-Min Tong, and Jia-Ming Li, Acta Phys. Sin. **45**, 13 (1996).
[23] A. Bar-shalom, J. Oreg, M. Klapisch, and T. Lehecka, Phys. Rev. E **59**, 3512 (1999).
[24] S.P. Zhu *et al.*, Institute of Applied Physics and Computational Mathematics research report, 2000 (unpublished).